J. Water Environ. Nanotechnol., 4(4): 321-332 Autumn 2019

ORIGINAL RESEARCH PAPER

Investigation and Comparison of Fluoride Adsorption Behavior on a Hybrid Material Containing Zirconium Dioxide Coated on γ-Alumina (60 and 90) and Their Initial Precursor in Aqueous Solution

Ramin Yavari

Material and Nuclear Fuel Scholl, Nuclear Science and Technology Research Institute, (NSTRI), Tehran, Iran

Received: 2019-06-28 Accepted: 2019-09-14 Published: 2019-11-01

ABSTRACT

In the present research work, zirconium oxide coated on activated alumina (Al_2O_3-90, Al_2O_3-60) were synthesized and used along with their pristine materials to investigate and compare the adsorption behavior of fluoride on them. These materials were characterized by BET and X-ray diffraction analyzer. The obtained results confirmed that the immobilization of ZrO_2 particles on the external surface pore of Al_2O_3-60 and Al_2O_3-90 has been performed successfully. The results of adsorption behavior study show that among these adsorbents, the synthesized hybrid material "Al_2O_3-60-ZrO_2" has high affinity toward the adsorption of fluoride ions from aqueous solution under ambient condition (36.62 $mg.g^{-1}$). Adsorption data in all of adsorbents were fitted with Langmuir model and the calculated E value shows that the chemical sorption process is a dominant mechanism in adsorption process. In the first 80 minutes of contact time, the maximum adsorption of fluoride was found to be for these synthesized hybrids" Al_2O_3-60-ZrO_2, Al_2O_3-90-ZrO_2". The adsorption rate of fluoride ions on these hybrid materials in spite of their initial material was almost independent on pH value in the range 3 to 8. The negative values of ΔG° indicate that the adsorption process of fluoride ions onto these adsorbents is exergonic and will proceed spontaneously. In addition, overall, the obtained results show that the prepared hybrid materials as adsorbents are promising and potential candidates for the adsorption and removal of trace amounts of fluoride from nuclear and chemical wastewater..

Keywords: *Fluoride ions; Adsorbent; ZrO_2; Al2O_3-60-ZrO_2; Al_2O_3-90-ZrO_2*

How to cite this article

*Yavari R. Investigation and Comparison of Fluoride Adsorption Behavior on a Hybrid Material Containing Zirconium Dioxide Coated on γ-Alumina (60 and 90) and Their Initial Precursor in Aqueous Solution. J. Water Environ. Nanotechnol., 2019; 4(4): 321-332. DOI: 10.22090/jwent.2019.04.00**

INTRODUCTION

The presence of fluoride in drinking water as a water contaminant has been a major health problem and it has been at the center of controversy for many years. Groundwater pollution by fluoride is as a result of weathering of fluoride-bearing rocks and minerals, volcanic eruption, and discharge of industrial effluents such as metal industry, semiconductor industry, uranium conversion facilities, glass, and fertilizer industry to the surface water [1]. Since drinking water is the major source of fluoride daily intake, depending on concentration of fluoride and the consumed amount, this element can be beneficial or harmful to the health of the organisms. According to the world health organization guideline, the maximum allowed amount of fluoride in drinking water has set within a certain range (between 0.5 and 1.0 ppm) to protect living beings [2]. Therefore, the presence of trace quantity of fluoride in drinking water is an essential component in the human diet and helps in the normal mineralization of bones and dental enamel formation. When its concentration exceeds from the mentioned level, mottling of teeth and deformation of bones (dental and skeletal fluorosis), brain damage, thyroid disorder and finally cancer

* Corresponding Author Email: *ryavari@aeoi.org.ir*

is observed [3-4]. Consequently, extensive research has been performed in the field of the removal of excess fluoride from wastewater. A literature survey reveals that to maintain fluoride within this permissible limit, various methods such as chemical precipitation, electrolysis, membrane process, ion exchange, and adsorption are considered as the main techniques [5-13]. Among them, adsorption is an easy, cost-effective and fast process that can act as the most effective technique for the reduction of fluoride concentration to below 1 ppm [13]. In this regard, many important adsorbents such as alumina, granular ceramic, zeolite, activated charcoal, carbonaceous, biosorbent, pyrophyllite, bauxite, chitosan and so on have been widely studied in recent years [14-25]. Considering the importance of fluoride removal from wastewater in the present decade, many researchers have been performed to explore, develop and improve the low-cost and effective adsorbents. Activated alumina as an amphoteric oxide with chemical formula Al_2O_3, is a well-known adsorbent for the economical and successfully removal of fluoride in low concentration. Principally, it is a porous aluminum oxide with a large surface area (usually between 240 and 300 $m^2.g^{-1}$) and the relative polarity which makes it suitable for adsorption of fluoride from aqueous solution [26]. However, due to its slow rate of adsorption, narrow operation pH range (5-6) and the limited regeneration capacity, the use of this material for the treatment of large volume of water has been restricted [5, 27-28]. One of the possible ways to solve this problem is the improvement of the surface of activated alumina with metal oxides which have a high fluoride adsorption capacity [27, 31-32]. The reported results show that the adsorption rate and capacity of fluoride on these modified materials were higher than their precursors. The literature survey shows that the zirconium oxide and some of its hybrid have been used for the removal of fluoride from wastewater [18, 33-35]. These adsorbents containing zirconium element have proved that their fluoride adsorption capacity is relatively high. Although the mixture of zirconium and aluminum oxide has been used for this purpose [36-38], no studies have been reported on the preparation and analytical applications of zirconium oxide coated on activated alumina for the use of them in the removal of fluoride from aqueous solution. Therefore, the aim of this study was to prepare, investigate and compare a new adsorbent based on zirconium oxide coated on the activated aluminum for the removal of fluoride from aqueous solution.

EXPERIMENTAL

Chemical and solutions

All the chemicals and reagents used in these experiments were of the analytical grade obtained from E. Merck or Fluka companies. Granular aluminum oxide-60 and 90 with the particle size of 0.063-0.2 mm (70-230 mesh) and different densities of 4 and 3.94 $g.cm^{-3}$, respectively, were used in this research work. A stock solution of fluoride (1000 ppm) was prepared by dissolving sodium fluoride in demineralized water (DMW). The solution was further diluted to the required concentrations (5-100 ppm). To adjust the solution pH, nitric acid and sodium hydroxide solutions with a concentration of 0.1 $mol.L^{-1}$ were used.

Preparation of zirconium oxide

Zirconium oxide nanoparticle was prepared via a sol-gel technique. Firstly, the proper amount of $ZrOCl_2 \cdot 8H_2O$ was added to 100 mL demineralized water with effective stirring (0.5 M $ZrOCl_2$_8H2O). Afterward, to prepare zirconium hydroxide's precipitation($Zr(OH)_4$), a little volume of 1M NaOH solution was gradually added to the above aqueous solution within 30 minutes in order to increase the pH value of the solution to 6.0-6.5 while the solution was continuously stirred at room temperature for 2 h. The formed precipitates were centrifuged and washed with distilled water several times. The obtained powder sample is finally dried overnight at 100 °C. The chemical reactions that occur are shown as follows.

Preparation of Al_2O3-60-ZrO_2 and Al_2O_3-90-ZrO_2

To prepare Al_2O_3-60-ZrO_2 and Al_2O_3-90-ZrO_2 adsorbents, a solution of 0.1M containing zirconium oxychloride as the zirconium precursor source was used. The preparation involved the following steps: first, 4g of each of Al_2O_3-60 and Al_2O_3-90 was added separately to 600 mL of 0,1M zirconium oxychloride solution. These solutions were kept under constant stirring at room temperature for 2h. The materials were then separated by filtration and dried overnight in an oven at 100 °C.

Apparatus

The Brunauer-Emmett-Teller specific surface area, pore specific volume and pore diameter of the samples were measured by nitrogen adsorption/

desorption at 77.4K using a Quantachrome nova station gas sorption analyzer. The XRD studies were made with a Philips model PW 1130/90. The quantitative determination of fluoride ions was carried out using fluoride selective electrode model ISTAK FOO1602. Waterbath shaker (model CH-4311, infors AG) was used throughout the work. The pH values of solution were measured with a Schott CG841 pH-meter (Germany).

Batch adsorption experiment

To study fluoride adsorption behavior on zirconium oxide, Al2O3-60, Al2O3-90 and zirconium oxide embedded on Al2O3-60 and Al2O3-90, the batch equilibrium method was applied. The adsorption capacities (qt) and the percentage of fluoride adsorption (p) were determined according to the following equations, respectively.

$$q_t = \frac{(C_o - C_t)*V}{W} \quad (1)$$

$$p = \left(1 - \frac{C_o}{C_e}\right) \times 100\% \quad (2)$$

where qt is the number of fluoride ions adsorbed onto adsorbent ($mg.g^{-1}$) at time t; Co is the concentration of initial fluoride ions (ppm); Ct is fluoride ions concentration after a certain period of time (ppm); V is the initial solution volume (L); and m is the adsorbent mass (g).

In order to study the effect of initial fluoride concentration on the adsorption of fluoride, 100 cm3 polyethylene bottles containing 100 mg of each of the adsorbents and 20 cm3 of fluoride solution with the initial concentration (Co) from 5 to 200 ppm and pH=5.5 were used. The bottles were capped and stored in a shaker operating at 298 K. The time of 24 hours and the stirring rate of 150 rpm was chosen to assure that the adsorption of fluoride was done completely. In addition, the effect of temperature on fluoride adsorption was studied at 288, 298, 308 and 318 K in the above-mentioned condition.

To investigate the effect of the solution pH value on fluoride adsorption at an initial concentration of 10 ppm, the number of hydronium ions in solution was adjusted at 10-3, 10-4, 10-5 and 10-6 M by adding negligible amount of concentrated nitric acid. Other conditions such as temperature, stripping rate and time were the same as above.

To study the effect of adsorbents mass on fluoride adsorption, the experiments were carried out by adding 25, 50, 75, 100, 125 and 150 mg of adsorbents into 20 mL of solution with pH=5.5 and initial fluoride concentration of 10 ppm.

Also, to study the effects of other anions such as sulfate and nitrate ions on fluoride adsorption, 20 mL fluoride solution containing an initial concentration of 10 ppm was mixed by 100 mg of adsorbents. The concentration of each of two anions (sulfate and nitrate ions) in the solution was adjusted at 0.001, 0.01, 0.1 and 1 M by adding a certain amount of sodium nitrate and sodium sulfate salts.

Finally, for the determination of equilibrium time, the times of 0.25, 0.5, 0.75, 1, 2, 5, 8 and 24 hours were selected and tested in the experimental conditions similar to the investigation of the effect of initial fluoride concentration on the adsorption of fluoride.

At the end of each test and after the separation of solids from the liquid phase by filtration through 0.45 µm membrane filters, the concentration of fluoride ions before and after equilibration was measured by ion-selective electrode method.

RESULT AND DISCUSSION

Characterization of synthesized materials

Fig. 1a and 1b exhibit N_2 adsorption/desorption isotherm curves of Al_2O_3 (60 and 90) and ZrO_2 embedded on Al_2O_3-60 and Al_2O_3-90, respectively. As can be seen, Al_2O_3-60 and Al_2O_3-90 samples show similar nitrogen absorption/desorption behavior while the typical isotherms of the Al_2O_3-60-ZrO_2, Al_2O_3-90-ZrO_2, and ZrO_2 samples are the same and show similar nitrogen absorption/desorption behavior, too. According to the original International Union of Pure and Applied Chemistry (IUPAC) classification, the convex plot to the relative pressure axis showed in Fig. 1a is characteristic of weak adsorbate-adsorbent interactions and it is most commonly associated with microporous adsorbents [39]. However, isotherms with H3 type hysteresis loops which depicted for all of adsorbents in Fig. 1b (Al_2O_3-60-ZrO_2, Al_2O_3-90-ZrO_2, and ZrO_2), are common features of type IV isotherms. This is commonly associated with the presence of mesoporosity structure in these adsorbents [40]. Therefore, the structure of microporous in Al_2O_3-60 and Al_2O_3-90 and mesoporosity structure in Al_2O_3-60-ZrO_2, Al_2O_3-90-ZrO_2, and ZrO_2 samples were confirmed by this method.

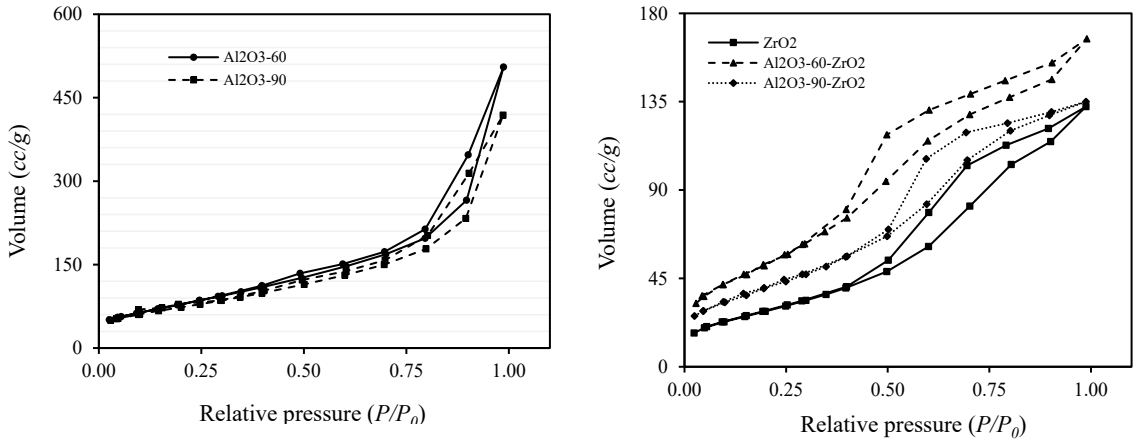

Fig. 1a and b. (1a) Nitrogen adsorption/desorption isotherms on Al_2O_3-60, Al_2O_3-90 at 77 K. (1b) Nitrogen adsorption/desorption isotherms on adsorbents Al_2O_3-60-ZrO_2, Al_2O_3-90-ZrO_2 and ZrO_2

Table 1. Physical properties (BET surface areas, pore size, and pore volume) of adsorbents.

No.	samples	BET surface area(m^2/g)	Pore size (nm)	Pore Volume (cm^3/g)
1	Al_2O_3-60	300.3	10.430	0.783
2	Al_2O_3-60-ZrO_2	207.9	4.983	0.259
3	Al_2O_3-90	268.1	6.495	0.275
4	Al_2O_3-90- ZrO_2	150.0	4.605	0.21
5	ZrO_2	109.8	6.187	0.205

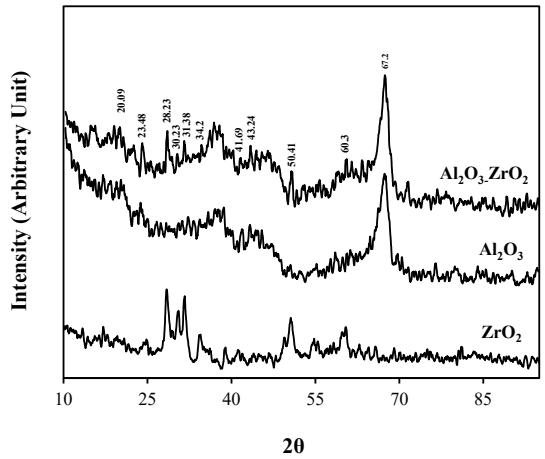

Fig. 2. XRD patterns of Al_2O_3, ZrO_2 and Al_2O_3-ZrO_2

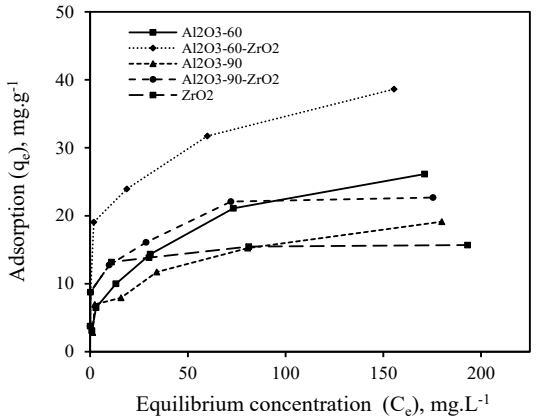

Fig. 3. Adsorption isotherms of fluoride ion onto adsorbents, pH = 5.5, t = 24 h, T = 298 K, adsorbent mass= 0.1 g, Agitation rate = 150 rpm.

The important physical properties such as specific surface areas and pore size distribution (including average pore diameter and pore volume) can be calculated using obtained N_2 adsorption/desorption data, BET (Brunauer, Emmett, and Teller) and BJH (Barrett, Johner, and Halenda) equations. The calculated parameters are shown in Table 1. As can be seen, the BET surface area of Al_2O_3-60 and 90 samples decreased after loading ZrO_2 onto them. This change can be due to the occupation of the Al_2O_3-60 and 90 microporous by the ZrO_2. In addition, we can observe that the pore diameter of Al_2O_3-60 and Al_2O_3-90 decreases after the loading of ZrO_2. This intimates that ZrO_2 particles are mostly positioned on the external surface pore of these new adsorbents and confirm the immobilization of ZrO_2 particles on Al_2O_3-60 and 90.

Crystalline structure and purity of the synthesized materials powder can be confirmed by powder X-ray diffractometer. The XRD patterns of Al_2O_3–ZrO_2 and its pristine material has been shown in Fig. 2. As can be seen, the characteristic and diffraction peaks of Al_2O_3 (20.09°, 23.48°, 41.69*°, 43.24°, 67.2°) and ZrO_2 (28.23°, 30.23°, 31.38°, 34.2°, 50.41°, 60.3°) match well with those of Al_2O_3 (Ref. code: JCPDS-00-013-0373) and ZrO_2 (Ref. code: JCPDS-01-088-1007), respectively, which diffraction intensity of Al_2O_3 and ZrO_2 peaks are become weaker and might be covered up in the XRD pattern of Al_2O_3–ZrO_2 shown in Fig. 2. This confirms the successful immobilization of ZrO_2 on Al_2O_3.

Adsorption isotherms

To acquire the maximum adsorption capacity of fluoride at an initial concentration range of 5-200 (ppm), the adsorption isotherms of fluoride on Al_2O_3-60, Al_2O_3-60-ZrO_2, Al_2O_3-90, Al_2O_3-90-ZrO_2 and ZrO_2 were studied. The obtained results have been depicted in Figs. 3 and 4. The changes in fluoride adsorption amount and percentage as a function of initial fluoride concentration on these adsorbents have been shown by these graphs. As can be seen in Fig. 3, for all of adsorbents, the amount of fluoride adsorption increases significantly in the range of low concentration of fluoride, while it increases gradually and reaches the nearly constant amount at an equilibrium concentration of about 150 ppm. Moreover, we can observe that the adsorption amount of fluoride on Al_2O_3-60 and 90 increases after loading ZrO_2 on them which indicates the improvement of the adsorption behavior of them. On the other hand, the results show that the maximum adsorption of fluoride was found to be 36.62 $mg.g^{-1}$ for Al_2O_3-60-ZrO_2 (q_e= 26.13 $mg.g^{-1}$). The order of adsorption amount of fluoride on these adsorbents is as follow;

Al_2O_3-60-ZrO_2 > Al_2O_3-60 > Al_2O_3-90-ZrO_2 > Al_2O_3-90 > ZrO_2

As shown in Fig. 4, the adsorption percentage of fluoride on these adsorbents decreases with increasing fluoride concentration. This phenomenon can be referred to the occupation of constant adsorption active site on these adsorbents by the fluoride ions at low concentration. Therefore, there will not exist the available site to adsorption of fluoride at higher concentrations which consequently gives rise to decrease the adsorption percentage of fluoride.

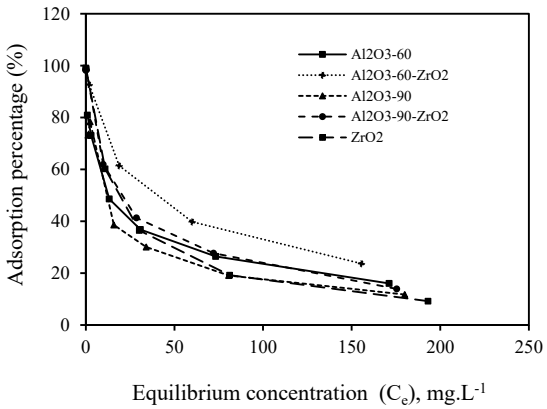

Fig. 4. Adsorption percentage of fluoride ions onto adsorbents, pH = 5.5, t = 24 h, T = 298 K, adsorbent mass= 0.1 g, Agitation rate = 150 rpm.

The adsorption equilibrium data of fluoride on these adsorbents were analyzed by the mathematical-statistical models such as Langmuir, Freundlich, and Dubinin–Radushkevich (D–R) equations which describe the distribution of the adsorbate species between two phases, liquid and solid phase, at equilibrium condition. These models have been established on a set of assumptions which are mostly depended on the heterogeneity/homogeneity of adsorbents, the type of coverage, and possibility of interaction between the adsorbate species. The description of a monolayer sorption mechanism with homogeneous sorption energies and a finite number of identical sites are validated by Langmuir model. The adsorption of solutes from a liquid to a solid surface on different sites with several adsorption energies is demonstrated by Freundlich model. At the same time, D–R model assumes that the surface of the adsorbents is heterogeneous [40]. The linear forms of these models are given in the following equations;

$$\textit{Langmuir Equation}: \quad \frac{C_e}{q_e} = \frac{1}{k_l q_m} + \frac{C_e}{q_m} \quad (3)$$

$$\textit{Frendlich Equation}: \quad lnq_e = lnk_f + \frac{1}{n} lnc_e \quad (4)$$

$$\textit{Dubinin} - \textit{Radshkevich Equation}: \quad \ln q_e = lnq_{DR} - B_{DR}\varepsilon^2 \quad (5)$$

where "q_m" is the maximum sorption capacity ($mg.g^{-1}$); "K_l" is the Langmuir sorption constant ($dm^3.mg^{-1}$) related to the energy of adsorption; "K_f ($mol^{1-n}.L^n.g^{-1}$)" and "n" are the Freundlich constants which indicate the adsorption capacity and the degree of dependence of sorption with equilibrium concentration, respectively. Moreover,

q_{DR} and B_{DR} (mol^2.J^{-2}) in E-R equation are (D–R) constants which related to the adsorption capacity and energy, and ε is the Polanyi potential which is expressed by;

$$\varepsilon = RTln\left(1+\frac{1}{C_e}\right) \quad (6)$$

where R is the gas universal constant (8.314 J.mol^{-1}.K^{-1}) and T is the absolute temperature (K). One of the important parameters of (D–R) equation which estimates the chemical or physical type of sorption process is E (kJ.mol^{-1}). This parameter can be calculated according to the following equation:

$$E = \frac{1}{\sqrt{2B_{DR}}} \quad (7)$$

The amount of obtained E from (D–R) equation can determine the type of sorption process. If 1< E < 8, a dominant mechanism is physical sorption. If 8<E<16, the chemical sorption will become a dominant mechanism. On the other hand, one of the significant parameters in Langmuir equation is the separation factor (R_L) which indicates the type of isotherm to be favorable ($0 < R_L < 1$) or unfavorable ($R_L > 1$). This parameter can be calculated by the following equation;

$$R_L = \frac{1}{1+bC_0} \quad (8)$$

Where C_0 (mg/L) is the highest initial solute concentration. The R_L indicates the type of isotherm to be favorable ($0 < R_L < 1$) or unfavorable ($R_L > 1$).

The value of all of the above mentioned constants is obtained from the slope and intercept of their linear plots of these equations (3-5). The linear plots of Langmuir, Freundlich and (D-R) equations were depicted in Figs. 5a to 5c, respectively. In addition, the calculated parameters were tabulated in Table 2.

As shown in Table 2, according to the highest correlation coefficients of the calculated linear regressions (R^2), the Langmuir model is the most suitable model which fits the equilibrium adsorption data of fluoride ions on the adsorbents. This indicates the homogeneous distribution of active sites on these adsorbents. The calculated maximum adsorption capacity (q_{max}) of fluoride by these models shows that Al_2O_3-60-ZrO_2 has high affinity toward fluoride ions (38.79 mg.g^{-1}). It implies that the prepared hybrid materials increase the adsorption of fluoride in comparison with their pristine material, Al_2O_3-60, Al_2O_3-90, and ZrO_2, (28.089, 20.161, 15.55 mg.g^{-1}). Moreover, the

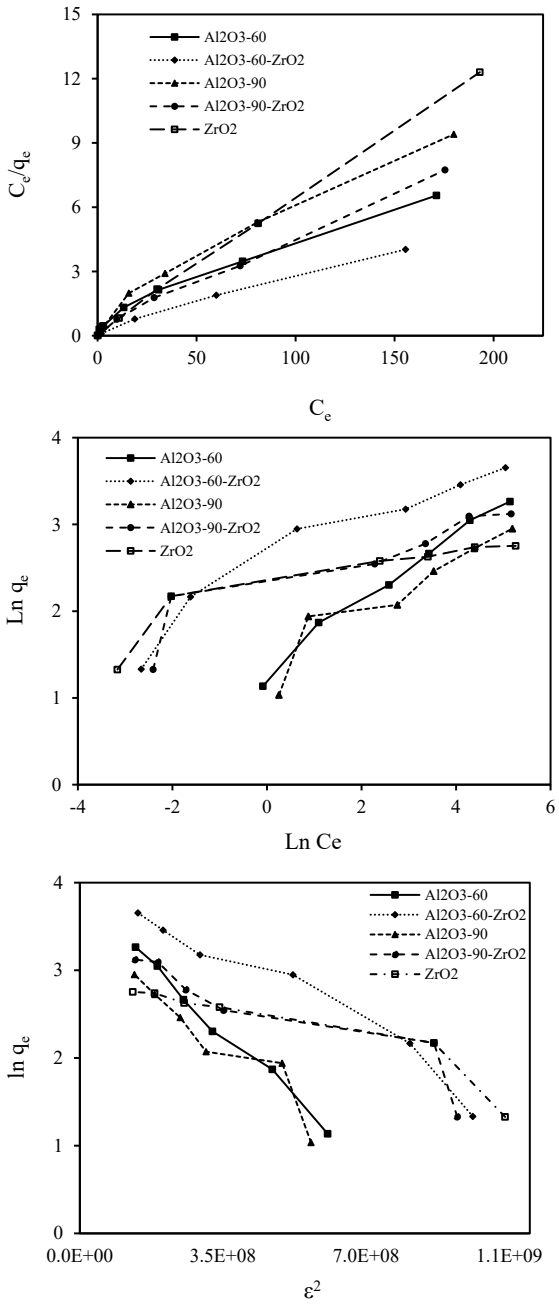

Fig. 5a, 5b, 5c. (4a) Langmuir, (4b) Freundlich and (4c) Dubinin-Radushkevich linear plots, respectively, for the adsorption isotherms of fluoride ions on adsorbents.

calculated values of R_L for all of adsorbents ($0 < R_L < 1$) indicate that adsorption is favorable. On the other hand, the value of the obtained E (1< E < 8) shows that a dominant mechanism in adsorption process is the chemical sorption.

Table 2. Langmuir, Freundlich and Dubinin-Radushkevich constants for adsorption of Fluoride ions on adsorbents.

Adsorbents	Langmuir isotherm			
	q_m(mg/g)	K_L(L/mg)	R_L	R^2
Al2O3-60	28.089	0.0228	0.18	0.9812
Al2O3-60-ZrO2	38.76	0.0032	0.61	0.9905
Al2O3-90	20.161	0.003	0.625	0.9804
Al2O3-90-ZrO2	23.148	0.0089	0.36	0.9952
ZrO2	15.55	0.006	0.45	0.9996
	Freundlich isotherm			
	K_F(mg/g)	n		R^2
Al2O3-60	3.622	2.508		0.9861
Al2O3-60-ZrO2	11.135	3.711		0.9180
Al2O3-90	3.515	3.014		0.8891
Al2O3-90-ZrO2	5.143	8.68		0.8637
ZrO2	8.335	6.95		0.8282
	Dubinin-Radushkevich isotherm			
	q_{DR}(mmol/g)	B_{DR}(mol^2/J^2)	E(KJ/mol)	R^2
Al_2O_3-60	2.50	4×10^{-9}	11.18	0.954
Al_2O_3-60-ZrO_2	2.98	3×10^{-9}	12.909	0.9552
Al_2O_3-90	1.58	4×10^{-9}	11.18	0.8945
Al_2O_3-90-ZrO_2	1.47	2×10^{-9}	15.81	0.8611
ZrO_2	1.35	18×10^{-10}	16.1	0.871

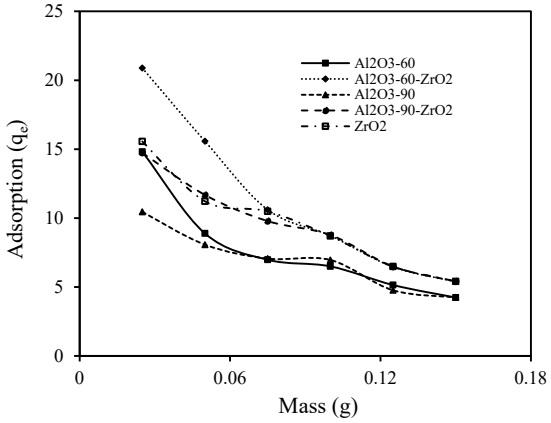

Fig. 6. Effect of adsorbents mass on fluoride ion adsorption onto adsorbents, pH = 5.5, t = 24 h, T = 298 K, Agitation rate = 150 rpm.

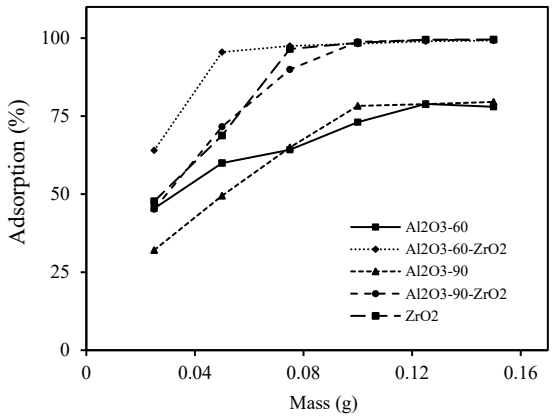

Fig. 7. Effect of adsorbents mass on fluoride ion adsorption percentage onto adsorbents, pH = 5.5, t = 24 h, T = 298 K, Agitation rate = 150 rpm.

Effect of Adsorbent Mass

One of the most effective parameters in the application of adsorbents for the removal of cations or anions from wastewater is the amount of adsorbent. If the amount of the used adsorbents in the elimination of elements is high, these materials cannot be used extensively as an adsorbent due to the economical total cost. Figs. 6 and 7 display the effect of the adsorbents mass (m) on the amount (q_e) and the percentage of fluoride adsorption, respectively. As can be seen in these figures, the percentage of fluoride adsorption increases and the amount of fluoride adsorption decreases with the increment of adsorbents concentration. This could be due to the availability of more adsorption sites on these adsorbents. In other words, in the fixed initial solute concentration, more adsorption sites are provided with increasing adsorbent dose [24].

Effect of pH

Because of the variation of ion species with the change of solution pH, investigation of the effect of hydronium ions on the ion adsorption is one of the other significant and dominant parameters. Fig. 8 shows the diagram of the effect of solution pH on the percentage of fluoride ion onto these adsorbents. As shown, the adsorption rate of fluoride ions on Al_2O_3-60-ZrO_2, Al_2O_3-90-ZrO_2 and ZrO_2 were

almost independent on pH value within the range 3 to 8 while the adsorption rate of fluoride ions on Al_2O_3-60 and Al_2O_3-90 was highly dependent on pH value. According to hydrofluoric acid dissociation constant ($6.8 \cdot 10^{-4}$ at 25 °C), fluoride species are present as HF and F^- at different pH values [12]. At low pH, where the concentration of hydronium ions is high, protonation of the sorbent's surface occurs. With the generation of positively charged sites, the electrostatic attraction force between these active sites and negative fluoride ions is increased and gives raised to the increase of the adsorption percentage of fluoride ions. At high pH, where the hydroxide ion concentration is high, adsorbent surface becomes negatively charged and increases the repellent force between the adsorbent´s surface and negatively fluoride ions. Thus, the decrease in fluoride adsorption percentage was observed.

Effect of nitrate and sulfate ions on the fluoride adsorption

The effects of coexisting anions such as nitrate and sulfate anions onto fluoride adsorption were investigated. The obtained results are represented in Figs. 9 and 10. As shown in Fig. 9, the adsorption percentage of fluoride for all of the adsorbents were independent of concentration nitrate ions for all of its concentration (0.001-1 M) while the considerable decrease of fluoride adsorption percentage was observed in all of adsorbents when sulfate ion was increased up to 0.1 M (Fig. 10). This is due to the affinity of these adsorbents toward sulfate ions and consequently, the competition between sulfate and fluoride ions toward the active site of adsorbents.

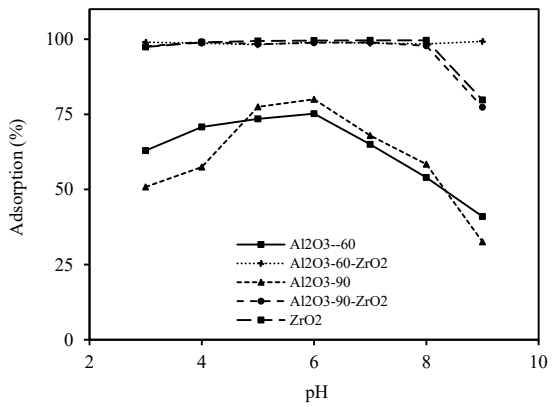

Fig. 8. Effect of pH values on the adsorption percentage of fluoride ions onto adsorbents, t = 24 h, T = 298 K, Adsorbent mass= 0.1 g, Agitation rate = 150 rpm.

Effect of contact time

Adsorption kinetics study is one of the important characteristics for the determination of the potential and efficiency application of adsorbents and for understanding the mechanism of adsorption process. Therefore, the adsorption percentage of fluoride onto all of adsorbents was studied as a function of contact time at initial fluoride concentration of 10 ppm. The obtained results are depicted in Fig. 11. As can be seen, the adsorption percentage of fluoride on Al_2O_3-60-ZrO_2, Al_2O_3-90-ZrO_2, and ZrO_2 increases quickly and reach to equilibrium time in the first 80 minutes of contact time while this time for Al_2O_3-60 and Al_2O_3-90 was obtained to be 8 hours. In addition, we can observe a negligible increase in the adsorption percentage of fluoride on all of adsorbents after this time. These two distinct parts could be assigned to the difference in mass transfer rate of fluoride ions

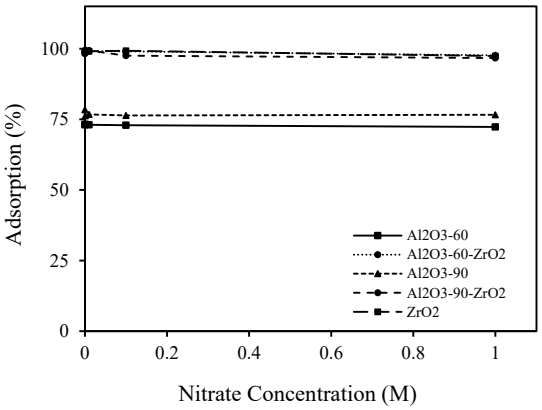

Fig. 9. Effect of nitrate ions on the fluoride ion adsorption percentage onto adsorbents, pH = 5.5, t = 24 h, T = 298 K, adsorbent mass= 0.1 g, Agitation rate = 150 rpm.

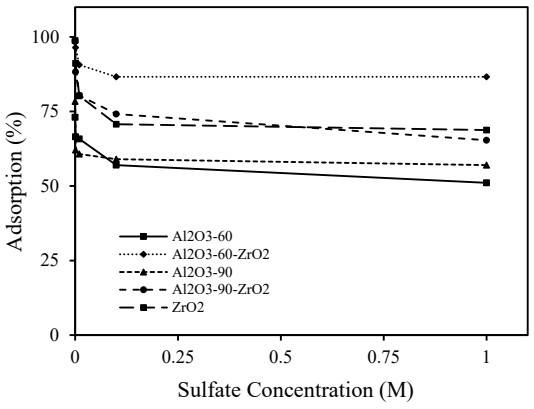

Fig. 10. Effect of sulfate ions on the fluoride ion adsorption percentage onto adsorbents, pH = 5.5, t = 24 h, T = 298 K, adsorbent mass= 0.1 g, Agitation rate = 150 rpm.

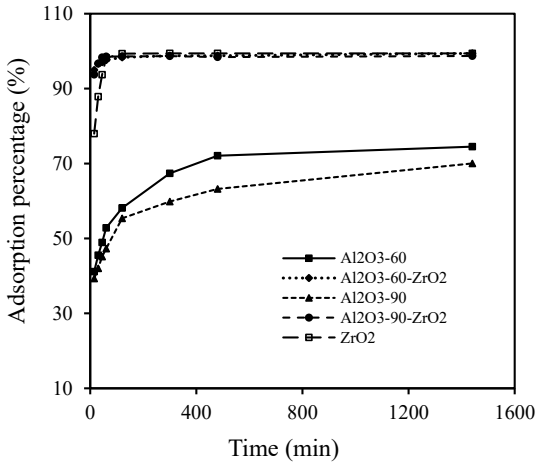

Fig. 11. Effect of contact time on fluoride ion adsorption percentage onto adsorbents, pH = 5.5, T = 298 K, adsorbent mass= 0.1 g, Agitation rate = 150 rpm.

in the first and final stages of adsorption process. The direct and easy availability of fluoride ions to the external adsorption sites of adsorbents could be the reason for the initial rapid adsorption. However, the next adsorption step which is slow is attributed to the slow diffusion rate of fluoride ions into the inner cavities and interlayer of adsorbents [17].

By using two common semiempirical kinetic models "the pseudo-first-order and pseudo-second-order equations" which are based on adsorption equilibrium capacity, the adsorption rate of ions on the adsorbents is studied. Therefore, these two models were used to simulate the kinetic adsorption data of fluoride on all of prepared adsorbents. In addition, linear arrangement of these equations is commonly used to investigate the validity of these models and to obtain their parameters. In this regard, the integrated and linearized forms of pseudo-first-order and pseudo-second-order are given as following equations 9 and 10, respectively:

$$\log(q_e - q_t) = \log q_e - \frac{k_1}{2.303}t \quad (9)$$

$$\frac{t}{q_t} = \frac{1}{k_2 q_e^2} + \frac{1}{q_e}t \quad (10)$$

Where q_e and q_t are the amounts of adsorbed fluoride ion concentration at equilibrium time and time t in mg.g^{-1}, k_1 and k_2 are the pseudo-first-order and pseudo-second-order constants expressed as min^{-1}and g.mg^{-1}.min^{-1}, respectively.

Figs. 12a and 12b show the linear plots of *log(qe–qt)* versus t and t/q_t versus t for all of the adsorbents.

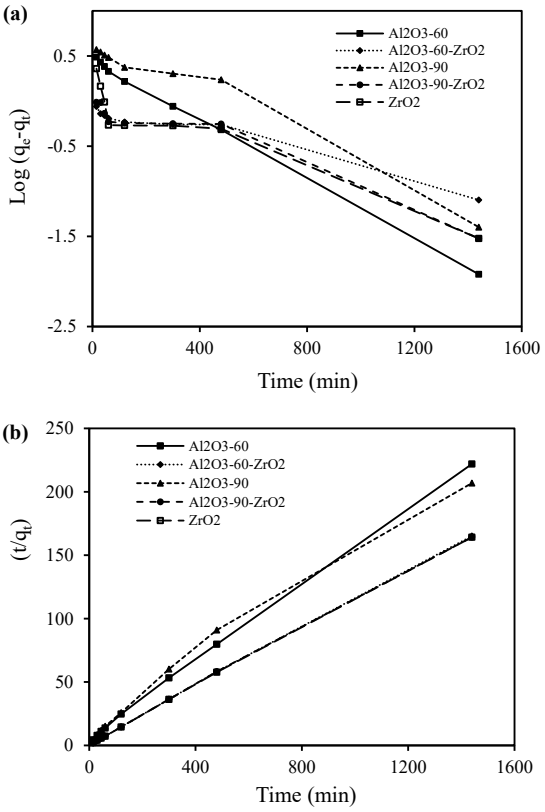

Fig. 12a and b, (11a) pseudo- first- order and (11b) pseudo-second- order linear plots for the adsorption of fluoride ions onto adsorbents.

From the slope and intercept of these linear plots, parameters like K_2, K_1, and q_e were obtained. These data accompany the amount of the calculated correlation coefficient (R^2) were listed in Table 3. By comparing the data of correlation coefficient of linear regression in Table 3, it indicates that the pseudo-second-order model is suitable model to describe the kinetic profile. And that is because of the good fitness of this model with the kinetic data. A similar phenomenon has also been seen in the adsorption of fluoride on other adsorbents [34, 41]. In other words, according to the higher correlation coefficient of linear regression, the interaction between the solute and adsorbents is the most probable limiting step for the sorption process. Moreover, higher value of K_2 Al_2O_3-60-ZrO_2 and Al_2O_3-90-ZrO_2 in comparison with three other adsorbents (Al_2O_3-60, Al_2O_3-90, and ZrO_2) indicates that the adsorption process achieves equilibration very quickly. This quickly equilibrium time confirms the ability of the synthesized hybrid material for application of them in the removal of fluoride from aqueous solution.

Table 3. The obtained kinetic parameters using Pseudo-first-order and Pseudo-second-order models

Sample	Concentration (mg/L)	Pseudo -first-order			Pseudo -second-order		
		k_1(1/min)	q_{e1}(mg/g)	R^2	k_2(g/mg min)	q_{e2}(mg/g)	R^2
Al_2O_3-60	10	0.0039	2.87	0.9785	0.068	6.6	0.999
Al_2O_3-60-ZrO2		0.0016	0.806	0.9509	0.120	8.72	0.999
Al_2O_3-90		0.0029	4.15	0.9678	0.047	7.05	0.988
Al2O3-90-ZrO2		0.0023	0.937	0.9358	0.109	8.77	0.999
ZrO_2		0.0025	1.19	0.8875	0.108	8.78	0.999

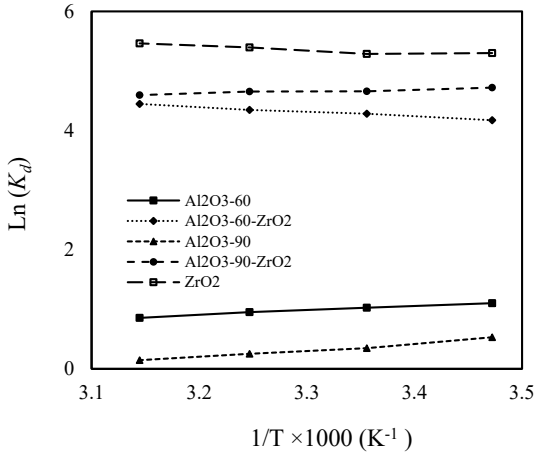

Fig. 13. Effect of temperature on adsorption of fluoride ions onto adsorbents.

Adsorption thermodynamics

To evaluate thermodynamic criteria and in order to determine which process will occur spontaneously, both Gibbs free energy and entropy factors must be calculated. Therefore, the effect of temperature on the adsorption behavior of fluoride ions has been studied in the range of 298- 328K. These thermodynamic parameters can be obtained by the following equations (11-12);

$$\Delta G^o = \Delta H^o - T\Delta S^o \quad (11)$$

$$LnK_d = \frac{\Delta S^o}{R} - \frac{\Delta H^o}{RT} \quad (12)$$

Where the $\Delta G°$ is the change in Gibbs free energy in j mol^{-1}, $\Delta S°$ is the change in the entropy

Table 4. Thermodynamics parameters of Fluoride ions on adsorbents at different temperatures in Kelvin.

sample	T(K)	ΔG° (KJ/mol)	ΔH° (KJ/mol)	ΔS° (J/Kmol)	R^2
Al_2O_3-60	303	-9.716	-6.02	-0.012	0.9916
	313	-9.839			
	323	-9.960			
	333	-10.082			
Al_2O_3-60-ZrO_2	303	-10.824	6.75	0.058	0.9923
	313	-11.404			
	323	-11.984			
	333	-12.564			
Al_2O_3-90	303	-0.8033	-9.56	-0.0289	0.9833
	313	-0.5143			
	323	-0.2253			
	333	-0.0637			
Al_2O_3-90-ZrO_2	303	-11.718	-2.87	0.0289	0.9198
	313	-12.009			
	323	-12.302			
	333	-12.594			
ZrO_2	303	-13.58	3.23	0.055	0.9279
	313	-14.142			
	323	-14.697			
	333	-15.252			

in jmol^{-1} and $\Delta H°$ is thechange in the enthalpy in j mol^{-1}, $\Delta S°$ is the change in the entropy in j mol^{-1}. T is the temperature in K, R is the universal gas constant (8.314 j.mol-1.K) and K_d is the distribution coefficient of elements which is calculated from the following formula;

$$K_d = (C_o - C_e) \times \frac{V}{m} \quad (13)$$

Where $C_o V$ and C_e are the concentration (ppm) of fluoride ions in the solution phase before and after the adsorption process, respectively, V is the volume of initial solution in mL, and m is the dry mass of the adsorbent in g. By drawing the linear plots of lnk_d vs. 1/T for all of the adsorbents and acquiring the slop and intercept of these linear graphs, the amount of ΔH° and ΔS° were obtained. Fig. 13 shows these linear graphs. The number of calculated parameters and the correlation coefficient of the linear regressions (R^2) are listed in Table 4.

As can be seen, the amounts of $\Delta G°$ for all of the adsorbents are negative. These negative values indicate that the adsorption process of fluoride ions onto these adsorbents is exergonic and will proceed spontaneously. In addition, it shows that the possibility of spontaneous reaction increases with temperature in the range of 298- 328K. The positive value of ΔH° in three adsorbents (Al_2O_3-60, Al_2O_3-90, and Al_2O_3-90-ZrO_2) suggests that the adsorption of fluoride on these adsorbents is an endothermic process while the negative value of ΔH° in Al_2O_3-60-ZrO_2 and ZrO_2 indicates that the adsorption process is exothermic. Although in some adsorbents, the amount of entropy (ΔH°>0) or enthalpy (ΔS°<0) is unfavorable, the reaction is spontaneous in all adsorbents. This means that the adsorption forces were strong enough to pass the energy barrier required by the reaction between the sorbent and adsorbates [42].

CONCLUSION

The results show that the synthesized hybrid materials "Al_2O_3-90-ZrO_2 and Al_2O_3-60-ZrO_2" have a high affinity toward the adsorption of fluoride ions from aqueous solution in comparison with their precursor. The maximum amounts of adsorbed fluoride onto the adsorbents were 26.13, 38.79, 19.12, 22.67 and 15.69 mg.g^{-1} for Al_2O_3-60, Al_2O_3-60-ZrO_2 Al_2O_3-90, Al_2O_3-90-ZrO_2 and ZrO_2, respectively. The homogeneous distribution of active sites on these adsorbents was confirmed by fitting adsorption data with Langmuir model. Moreover, the chemical sorption process as a dominant mechanism in adsorption process by calculated E value and correspondence of the adsorption data with the pseudo-second-order kinetics model was proved. The maximum adsorption of fluoride in the first 80 minutes of contact time for the synthesized hybrids was achieved which indicating proper adsorption rate and their potential and efficiency application. The adsorption rate of fluoride ions on these hybrid materials in spite of their initial material was almost independent on pH value within the range 3 to 8. Overall, based on the obtained experimental results, we can claim that the prepared hybrid materials as adsorbents are promising and potential candidates for the adsorption and removal of trace amounts of fluoride from chemical wastewater.

CONFLICTS OF INTEREST

There are no conflicts to declare.

REFERENCES

1. Goswami, A., Purkait, M. K. Chem. Eng. Res. Des. 2012, Vol. 90,no.12, pp. 2316–2324.
2. World Health Organization WHO. Guidelines for drinking-water quality, 4nd ed., World Health Organization, Geneva; Chapter 12. 2011.
3. Lounici, H., Addour, L., Belhocine, D., Grib, H., Nicolas, S., Bariou, B. Desalination. 1997, vol. 114, no. 3 pp. 241–251.
4. Hichour, M., Persin, F., Sandeaux, J., Gavach, C. Sep. Purif. Technol. 2000, vol. 18, no. pp. 1–11.
5. Meenakshi, R. C. Maheshwari, J. Hazard. Mater. 2006, vol. 137, no. 1, pp. 456–463.
6. Mohapatra. M., Anand, S., Mishra, B. K., Giles, D. E., Singh, P. J. Environ. Manage. 2009, vol. 91, no.1, pp. 67–77.
7. Sehn, P. Desalination. 2008, vol. 223, pp. 73–84.
8. Verma, N., Verma, H., Meena, R. C. Inter. J. Pharm. Res. Bio. Sci. 2014, VOL. 3, no. , pp. 328-351.
9. Habuda-Stanić, M., Ravančić, M. E., Flanagan, A. Materials. 2014, vol. 7, no. 9, pp. 6317-6366.
10. Ghosh, D., Medhi, C. R., Purkait, M. K. Chemosphere. 2008, vol. 73, no. 9, pp.1393-1400.
11. Shimelis, B., Zewge, F., Chandravanshi, B. S. Bull. Chem. Soc. Ethiop. 2006, vol. 20, no. 1, pp. 17-34.
12. Tomar, V., Kumar, D. Chem. Cen. J. 2013, Vol. 7, no. 1, pp. 511-515.
13. Pietrelli, L. Annali. Di. Chimica. 2005, vol. 95, no. 5, pp. 303–312.
14. Lee, G., Chen, C., Yang, S. T., Ahn, W.S. Micropo. Mesopo. Mat. 2010, vol. 127, no. 1-2, pp. 152–156.
15. Chen, N., Zhang, Z., Feng, C., Sugiura, N., Li, M., Chen, R. J. Colloid. Interf. Sci. 2010, vol. 348, No. 2, pp. 579–584.
16. Emmanuel, K. A., Ramaraju, G., Rambabu, A., Rao, V. Rasayan. J. Chem. 2008, vol. 4, no. 1, pp. 802–818.
17. Sun, Y., Fang, Q., Dong, J., Cheng, X., Xu, J. 2011, vol. 277, no. 1, pp. 121–127.
18. Dou. X., Mohan, D., Pittman, Jr. C.U., Yang, S. Chem. Eng. J.

2012, vol. 198–199, pp. 236–245.
19. Babaeivelni, K., Khodadoust, A. P. J. Colloid. Interf. Sci. 2013, vol. 394, pp. 419–427.
20. Raichur, A. M. Basu, J. M. Sep. Purif. Technol. 2001, vol. 24, No. 1-2, pp. 121–127.
21. Abe, I., Iwasaki, S., Tokimoto, T., Kawasaki, N., Nakamura, T., Tanada, S. J. Colloid. Interf. Sci. 2004, vol. 275, no. 1, pp. 35–39.
23. Mohan, S. V., Ramanaiah, S. V., Rajkumar, B., Sarma, P. N. J. Haz. Mat. 2007, vol. 141, no. 3, pp. 465-474.
23. Goswami, S., Dey, S., Ghosh, U. C. J. Chem. Environ. Res. 2004, vol. 13, pp. 117–126.
24. Sajidu, S., Kayira, C., Masamba, W., Mwatseteza, J. Environ. Nat. Resour. Res. 2012, vol. 2, no. 3, pp. 1–9.
25. Viswanathan, N., Meenakshi, S. Colloids. Surf. B. 2009, vol. 72, no. 1, pp. 88–93.
26. Waghmare, S. S., Arfin, T. J. Biol. Chem. Chron. 2015, vol. 2, no. 1, pp. 1-11.
27. Teng, S. X., Wang, S. G., Gong, W. X., Liu, X.W., Gao, B.Y. J. Haz. Mater. 2009, Vol. 168, no. 2-3, pp. 1004–1011.
28. Maliyekkal, S. M., Sharma, A. K., Philip, L. Manganese-oxide-coated alumina: a promising sorbent for defluoridation of water. Water. Res. 2006, vol. 40, no. 1, pp. 3497–3506.
29. Bansiwal, A., Pillewan, P., Biniwale, R. B., Rayalu, S. S. Micropo. Mesopo. Mat. 2010, vol. 129, no. 1-2, pp. 54–61.
30. Maliyekkal, S. M., Shukla, S., Philip, L., Nambi, I. M. Chem. Eng. J. 2008, vol. 140, no. 1-3, pp. 183–192.
31. Camacho, L. M., Torres, A., Saha, D., Deng, S. J. Colloid. Interf. Sci. 2010, vol. 349, no. 1, pp. 307–313.
32. Kamble, S. P., Deshpande, G., Barve, P. P., Rayalu, S., Labhsetwar, N. K., Malyshew, A., Kulkarni, B.D. Desalination. 2010, vol. 264, no. 1-2, pp. 15–23.
33. Biswas, K., Bandhoyapadhyay, D., Ghosh, U. Adsorption. 2007, vol. 13, No. 1, pp. 83–94.
34. Liao, X. P., Shi, B. Environ. Sci. Technol. 2005, vol. 39, no. 12, pp. 4628–4632.
35. Janardhana, C. Indian. J. Chem. Technol. 2007, vol. 14, pp. 355-361.
36. Viswanathan, N., Sundaram, C. S., Meenakshi, S. J. Hazard. Mater. 2009, vol. 161, no. 1, pp. 423–430.
37. Zhu, J., Lin, X., Wu, P., Zhou, Q., Luo, X. Appl. Sur. Sci. 2015, vol. 357, pp. 91–100.
38. Adak, M. K., Mondal, B., Dhak, P., Sen, S., Dhak, D. Adv. Wat. Sci. Tech. 2017, vol. 4, no. 1, pp. 1-10
39. Sing, K., Everett, D., Hau, R., Moscou, L., Pierotti, R., Rouquero, J., Siemieniewska, T. Pure. Appl. Chem. 1985, vol. 57, pp. 603–619.
40. Yavari, R., Asadollahi, N., Mohsen, M. A. Prog. Nucl. Energy. 2017, vol. 100, pp. 183-191.
41. Sivasamy, A., Singh, K. P., Mohan, D., Maruthamuthu, M. J. Chem. Technol. Biotechnol. 2001, Vol. 76, no. 7, pp. 717-722.
42. Liu, J., Wan, L., Zhang, L., Zhou, Q. J. Colloid. Interf. Sci. 2011, vol. 364, no. 2, pp.490–496.